NLR locus-mediated trade-off between abiotic and biotic stress adaptation in Arabidopsis

Hirotaka Ariga[1]†, Taku Katori[1]‡, Takashi Tsuchimatsu[2]‡, Taishi Hirase[3]‡, Yuri Tajima[3], Jane E. Parker[4], Rubén Alcázar[5], Maarten Koornneef[6], Owen Hoekenga[7]†, Alexander E. Lipka[7]†, Michael A. Gore[8]†, Hitoshi Sakakibara[9], Mikiko Kojima[9], Yuriko Kobayashi[10]†, Satoshi Iuchi[10], Masatomo Kobayashi[10], Kazuo Shinozaki[11], Yoichi Sakata[1], Takahisa Hayashi[1], Yusuke Saijo[3,12] and Teruaki Taji[1]

[1]Department of Bioscience, Tokyo University of Agriculture, Tokyo 156-8502, Japan. [2]Department of Biology, Chiba University, Chiba 263-8522, Japan. [3]Grad. School of Biological Sciences, Nara Institute for Science and Technology, Ikoma 630-0192, Japan. [4]Dept. of Plant-Microbe Interactions, Max-Planck Institute for Plant Breeding Research, D-50829 Cologne, Germany. [5]Dept. Plant Biology, University of Barcelona, 08028 Barcelona, Spain. [6]Dept. of Plant Breeding and Genetics, Max-Planck Institute for Plant Breeding Research D-50829 Cologne, Germany. [7]United States Department of Agriculture, Agricultural Research Service (USDA-ARS), Ithaca, New York 14853 [8]United States Department of Agriculture, Agricultural Research Service (USDA-ARS), Maricopa, AZ 85138, USA. [9]Plant Productivity Systems Research Group, RIKEN Center for Sustainable Resource Science, Kanagawa 230-0045, Japan. [10]RIKEN BioResource Center, Ibaraki, 305-0074 Japan. [11]Gene Discovery Research Group,

RIKEN Center for Sustainable Resource Science, Kanagawa 230-0045, Japan. [12]JST PRESTO, Ikoma 630-0192, Japan.

†Present address: Division of Plant Sciences, Institute of Agrobiological Science, NARO, Ibaraki 305-8602, Japan. (H.A.); Cayuga Genetics Consulting Group LLC, Ithaca, New York 14850, USA. (O.H.); University of Illinois, Department of Crop Sciences, Urbana, IL 61801, USA. (A.E.L); Plant Breeding and Genetics Section, School of Integrative Plant Science, Cornell University, Ithaca, New York 14853, USA. (M.A.G.); Faculty of Applied Biological Sciences, Gifu University, Gifu 501-1193, Japan. (Y.K.)

‡These authors contributed equally to this work.

Osmotic stress caused by drought, salt or cold decreases plant fitness. Acquired stress tolerance defines the ability of plants to withstand stress following an initial exposure[1]. We found previously that acquired osmotolerance after salt stress is widespread among *Arabidopsis thaliana* accessions[2]. Here, we identify *ACQOS* as the locus responsible for acquired osmotolerance. Of its five haplotypes, only plants carrying Group 1 *ACQOS* are impaired in acquired osmotolerance. *ACQOS* is identical to *VICTR*, encoding a nucleotide-binding leucine-rich repeat (NLR) protein[3]. In the absence of osmotic stress, Group 1 *ACQOS* contributes to bacterial resistance. In its presence, *ACQOS* causes detrimental autoimmunity, thereby reducing osmotolerance. Analysis of natural variation at the *ACQOS* locus suggests that functional and non-functional *ACQOS* alleles are being maintained due to a trade-off between biotic and abiotic stress adaptation. Thus, polymorphism in certain plant *NLR* genes might be influenced by competing environmental stresses.

Natural genetic variation has facilitated the identification of genes underlying complex traits such as growth, flowering, and stress tolerance, while creating opportunities for adaptation to changing environmental conditions[4]. Studies of several hundred *A. thaliana* accessions have provided new insights into genome evolution, differentiation among geographic populations and selective mechanisms that shape complex trait variation in nature[5]. Plants have evolved the ability to acclimatize to various stresses after initial exposure to a related stress cue[1]. A large-scale analysis of 350 *A. thaliana* accessions revealed extensive variation in acquired osmotolerance upon mild salt exposure[2]. When 7-day-old seedlings were pre-exposed to 100 mM NaCl for 7 d (acclimation period), the *A. thaliana* accessions Bu-5 and Bur-0, but not Col-0 or Wl-0, acquired osmotolerance to 750 mM sorbitol[2] (**Fig. 1a**). Using the progeny of a

Bu-5 × Col-0 cross, we mapped a single locus on chromosome 5, which we named acquired osmotolerance (*ACQOS*).

Here, we resolved the *ACQOS* locus to a 100-kilobase (kb) region on chromosome 5 containing 24 annotated genes (**Supplementary Fig. 1**). We then developed two BC_5F_3 near-isogenic lines, NIL-Col-0 and NIL-Bu-5, which carried different sized small chromosomal segments from Bu-5 containing the *ACQOS* region in the genetic background of Col-0. Retention of acquired osmotolerance in NIL-Bu-5 but not NIL-Col-0 narrowed down the *ACQOS* locus to a 67-kb region (**Fig. 1b** and **Supplementary Fig. 2a**). To investigate whether the *ACQOS* locus accounts for species-wide variation in acquired osmotolerance, we performed a genome-wide association study (GWAS) using 179 accessions (**Supplementary Table 1**). This revealed a significant ~200-kb-wide peak on chromosome 5 that coincided with large linkage disequilibrium patterns within ± 500 kb of the *ACQOS* locus, consistent with the fine mapping data (**Fig. 1c**). To identify polymorphisms in the region, we constructed a BAC library derived from Bu-5 genomic DNA and sequenced a BAC clone containing the region. Sequencing revealed a 17-kb deletion in Bu-5. In the corresponding region, Col-0 has a tandem repeat of four *Toll and interleukin1 receptor–nucleotide binding–leucine-rich repeat* (*TIR-NLR*) genes (*NLR1–NLR4*; *NLR2* encodes a truncated, apparently non-functional protein), whereas Bu-5 has one *TIR-NLR* gene (**Fig. 1b** and **Supplementary Fig. 3**). We tested whether this single $NLR^{Bu\text{-}5}$ confers osmotolerance in Bu-5 or one or more of the four Col-0 *NLRs* impairs acquired osmotolerance, by introducing different *NLRs* into Col-0 and NIL-Bu-5. In these complementation assays, $NLR^{Bu\text{-}5}$ did not confer acquired osmotolerance in the Col-0 background (**Supplementary Fig. 4**). By contrast, Col-0 *NLR4*, but not *NLR3*,

abolished osmotolerance in the NIL-Bu-5 background (**Fig. 1d** and **Supplementary Fig. 4**). Also, disruption of *NLR4* but not *NLR2* or *NLR3* in Col-0 by T-DNA insertion conferred acquired osmotolerance equivalent to that of NIL-Bu-5 (**Fig. 1e** and **Supplementary Fig. 5**). Therefore, Col-0 *NLR4* suppresses the acquired osmotolerance of Bu-5. These results suggest that *NLR4* is the *ACQOS* locus underlying variation in acquired osmotolerance.

Col-0 *ACQOS* was described previously as *VICTR* (*VARIATION IN COMPOUND TRIGGERED ROOT* growth response), which mediates root growth arrest induced by the small molecule [5-(3,4-dichlorophenyl)furan-2-yl]-piperidine-1-ylmethanethione (DFPM) in Col-0[3]. ACQOS/VICTR protein associated with and required the TIR-NLR immunity regulators Enhanced Disease Susceptibility1 (EDS1) and Phytoalexin-Deficient4 (PAD4) for DFPM-induced immunity and antagonism of certain osmotic stress responses mediated by the hormone abscisic acid (ABA)[3,6]. In plants and animals, NLR proteins are typically immune sensors for pathogen molecules or pathogen-induced modifications of host cell components[7]. There are 104 annotated *TIR-NLR*s in the genome of *A. thaliana* Col-0. The closest homolog of *ACQOS* in Col-0 is *NLR3*, which is also missing in Bu-5 (**Supplementary Fig. 6**). In Col-0, *ACQOS* gene expression was induced predominantly in roots in response to osmotic stress (**Fig. 1f**, **g**). To investigate whether *ACQOS* expression levels influence the extent of acquired osmotolerance, we exploited an osmotic stress-inducible *ACQOS*-overexpression line identified among the *ACQOS* transgenic lines in the NIL-Bu-5 background (see **Fig. 1d**). Osmotic stress–inducible overexpression of *ACQOS* (line #3), without a significant increase in basal expression, rendered the seedlings more sensitive to osmotic stress than other less strongly inducible lines or Col-0 plants (**Supplementary Figs. 7**). In

addition, F_1 progeny of Col-0 × NIL-Bu-5 showed a partial breakdown of acquired osmotolerance (**Supplementary Fig. 8**). These results show that *ACQOS* suppresses the acquisition of osmotolerance in a dose-dependent manner.

To explore nucleotide variation at the *ACQOS* locus, we performed PCR-based cloning and Sanger sequencing of a ~23-kb genomic region encompassing the *ACQOS* gene in 79 *A. thaliana* accessions. We chose Sanger sequencing because standard Illumina short-read sequencing is often unreliable if there are large deletions, insertions or tandem repeats, as found in the *ACQOS* region. Based on the pattern of indels and tandem repeats, we classified the tested accessions into five *ACQOS* haplogroups (Groups 1–5) (**Fig. 2a** and **Supplementary Fig. 9a**). Group 1, which includes Col-0, was rare (10%), whereas Group 4 including Bu-5, and Group 5 were most frequent (72%; **Fig. 2b**). As expected from the prominent GWAS peak around the *ACQOS* locus (**Fig 1c**), we found a strong correlation between the haplogroup and acquired osmotolerance: Groups 2–5 displayed osmotolerance, whereas Group 1 did not (**Fig. 2c** and **Supplementary Fig. 2b**). Notably, Group 2 carrying polymorphisms in the *ACQOS* gene (**Fig. 2d**) had acquired osmotolerance (**Fig. 2c** and **Supplementary Fig. 2b**). This suggests that nucleotide substitutions between the Group 1 and 2 *ACQOS* genes explain the presence or absence of acquired osmotolerance. To test this possibility, we introduced the corresponding *ACQOS* genes from Col-0 (Group 1) or Rou-0 (Group 2) into *ACQOS* knockout mutants. In these complementation experiments, Group 1 but not Group 2 *ACQOS* strongly reduced acquired osmotolerance (**Fig. 2e** and **Supplementary Fig. 2c**), indicating that the nucleotide substitutions render Group 2 *ACQOS* non-functional in osmotolerance suppression.

To explore haplotype and allelic diversity at the *ACQOS* locus, we conducted a phylogenetic analysis of the tandemly duplicated *ACQOS* homologs, including those from *Arabidopsis lyrata* as an outgroup[8] (**Fig. 2f**). The corresponding region of *A. lyrata* contains three *TIR-NLR* genes which differ from *A. thaliana*, suggesting that this locus has evolved independently after species divergence (**Supplementary Fig. 9b**). The phylogeny revealed that *NLR* genes within the *ACQOS* locus fall into two major clades, one containing Group 4 *NLR* and an *A. lyrata* homolog (named haplogroup A) and the other containing Group 5 *NLR* (named haplogroup B) (**Fig. 2f**). *NLR1* in Groups 1–3 appears to be closest to the $NLR^{\text{Group 4}}$, whereas *NLR3* of Groups 1–3 and *ACQOS* belong to the same clade as $NLR^{\text{Group 5}}$. These results suggest that two divergent single-copy *NLR* haplogroups (A and B) evolved initially, and that *NLR3* and *ACQOS* originated through tandem duplication in the haplogroup A. Nucleotide diversity at *ACQOS*, especially in the LRR domain, is higher than the genome-wide average[9] and that of *NLR1-NLR3* in the *ACQOS* locus, and is associated with an excess of non-synonymous over synonymous substitutions between Group 1 and Group 2 *ACQOS* genes, suggesting diversifying selection (**Fig. 2d**; **Supplementary Fig. 10**). In one of three *ACQOS* high-diversity regions, polymorphisms were shared between *ACQOS* and $NLR^{\text{Group 5}}$, suggesting that heterologous recombination due to unequal crossing over or gene conversion between $NLR^{\text{Group 5}}$ and *ACQOS* may have contributed to the high level of variation in the *ACQOS* gene (**Supplementary Figs. 11, 12**). Also, because *A. thaliana* Group 3 accessions showed acquired osmotolerance, we reasoned that this trait is due to a non-functional *ACQOS* gene. The 3' portion of Group 3 *NLR3* is more closely related to that of Group 1 *ACQOS* than to Group 1 or 2 *NLR3*. It seems that deleting the majority of *ACQOS* 5' region by gene fusion with *NLR3* suppressed

155 *ACQOS* function in Group 3 (**Supplementary Fig. 13**). Our data suggest that acquired
156 osmotolerance was impaired when *ACQOS* originated, and was then restored in *A.*
157 *thaliana* after repeated rearrangements, recombination and/or mutations at the *ACQOS*
158 locus, giving rise to the haplotype groups 2, 3 and 5.

159 In pathogen-triggered TIR-NLR immunity and autoimmunity, EDS1/PAD4 nuclear
160 complexes transcriptionally reprogram cells for pathogen resistance via salicylic acid
161 (SA) and SA-independent pathways[10,11]. When exposed to osmotic stress, SA
162 accumulation and the defence marker genes *PR1* and *EDS1* (SA-dependent) and *PR2*
163 (SA-independent[12]) were strongly induced in Col-0 but not in NIL-Bu-5 plants (**Fig. 3a,**
164 **b**). These results suggest that immune responses are de-repressed under osmotic stress
165 in the presence of *ACQOS*. Given that SA antagonizes ABA signalling in *A. thaliana*[13],
166 we tested for roles of *EDS1*, *PAD4* and SA in the impaired Col-0 acquired
167 osmotolerance. Notably, Col-0 plants displayed acquired osmotolerance when *EDS1* or
168 *PAD4* were mutated (**Fig. 3c, d**). Consistent with this, Group1 *ACQOS* failed to
169 suppress acquired osmotolerance at 28 ºC, at which TIR-NLR and EDS1/PAD4
170 immune responses are compromised in several *A. thaliana* accessions[14]
171 (**Supplementary Fig. 14**). By contrast, acquired osmotolerance remained suppressed in
172 mutants of *EDS5*, *SID2* or *NPR1*, encoding an SA transporter, an SA biosynthetic
173 enzyme (Isochorismate Synthase 1) and a SA signalling regulator, respectively (**Fig. 3c,**
174 **d**), pointing to SA independence of ACQOS suppression of osmotolerance. We further
175 tested whether ACQOS relies on RAR1 and SGT1, which facilitate stable NLR
176 accumulation and function[15]. Acquired osmotolerance was observed in *rar1* and *sgt1b*
177 plants, albeit to a lesser extent in the latter compared with *rar1*, *eds1*, and *pad4* plants,
178 possibly due to the retention of *SGT1a* (**Fig. 3c, d**). None of these four genes was

179 associated with acquired osmotolerance in our GWAS (**Fig. 1c**). Our findings suggest
180 that under osmotic stress, de-repression of TIR-NLR ACQOS-mediated defences via
181 EDS1/PAD4 leads to a loss of acquired osmotolerance. Misactivated immunity often
182 results in stunted growth and necrotic lesioning[14] and *NLR* genes have been reported to
183 influence plant development, growth and cold tolerance in *Arabidopsis thaliana*[16,17].
184 Under our conditions, plant growth was largely indistinguishable between Col-0, Bu-5,
185 NIL-Bu-5 and *acqos* knockout plants when transferred to 4 ºC after 100 mM NaCl
186 treatment. These results suggest that ACQOS de-repression connects to auto-immunity
187 specifically under osmotic stress conditions. Osmotic tolerance often depends on ABA,
188 which increases with osmotic stress. Induced ABA accumulation and expression of the
189 ABA-responsive genes *RAB18, RS6* and *NCED3* was higher in NIL-Bu-5 than Col-0
190 when plants were exposed to high osmotic stress, although their induction was not
191 detectable during initial salt stress (**Supplementary Fig. 15a, b**). To assess the role of
192 ABA in acquired osmotolerance, we introduced mutations into the NIL-Bu-5
193 background: *aba2-1*[18] (*aba2-1*_NIL-Bu-5) and *nced3-2*[19] (*nced3-2*_NIL-Bu-5) which
194 are defective in ABA biosynthesis, or *abi1-1*[20,21] (*abi1-1*_NIL-Bu-5) which is
195 ABA-insensitive. Unexpectedly, acquired osmotolerance in NIL-Bu-5 was unaffected
196 by these mutations (**Supplementary Fig. 15c**), indicating that the osmotolerance
197 suppressed by *ACQOS* is independent of ABA.
198 The observed species-wide variation in acquired osmotolerance, in particular
199 retention of the *ACQOS* allele that disables this trait, might be explained if *ACQOS* has
200 fitness benefits under certain conditions. As a trade-off often occurs between biotic and
201 abiotic stress adaptation[22], we tested whether Group 1 *ACQOS* influences plant
202 immunity. In *A. thaliana*, acquired osmotolerance and pathogen resistance are not

203 necessarily correlated at the level of accessions[23], likely reflecting complex genetic
204 interactions in the control and/or coordination of the two traits. We therefore compared
205 Col-0 and NIL-Bu-5 plants to assess directly a role for Group 1 *ACQOS* in defence
206 responses. Recognition of bacterial flagellin (flg22 epitope), a pathogen-associated
207 molecular pattern (PAMP), and subsequent defence activation is critical in bacterial
208 resistance and largely conserved in higher plants[24], with a degree of species-wide
209 variation in *A. thaliana*[25]. We tested flg22-triggered induction of the defence markers
210 *PROPEP3* and *NHL10* in Col-0 and NIL-Bu-5 plants, and in *efr fls2* plants that lack the
211 flg22 receptor FLS2 and are insensitive to flg22[26]. Induction of these two markers in
212 response to flg22 was lower in NIL-Bu-5 plants compared to Col-0 plants, suggesting
213 that flg22-triggered defences are lowered in the absence of *ACQOS* (**Fig. 3e**). As
214 accumulation of FLS2 and its coreceptor BAK1[27] was intact in NIL-Bu-5 plants
215 (**Supplementary Fig. 16**), this implies a role for ACQOS in defence signalling
216 downstream of PAMP perception. To assess the biological significance of this finding,
217 we tested whether loss of *ACQOS* influences bacterial resistance. NIL-Bu-5 and Col-0
218 plants were indistinguishable in basal resistance (without flg22 pretreatment) to virulent
219 *Pseudomonas syringae* pv. *tomato* strain DC3000 (*Pst* DC3000) (**Fig. 3f**). Following
220 flg22 pretreatment, however, NIL-Bu-5 plants exhibited lower suppression of bacterial
221 growth compared to Col-0 plants which strongly reduced bacterial growth, as described
222 previously[28] (**Fig. 3f**). These data suggest that Group 1 *ACQOS* is required for full
223 activation of FLS2-mediated bacterial resistance, and that a contribution to this key
224 branch of PAMP-triggered immunity might present an advantage for retaining
225 functional *ACQOS*.

Polymorphism associated with rearrangements and mutations in the single *ACQOS* locus implies that acquired osmotolerance has evolved independently several times by *ACQOS* disruption, despite its potential for compromising immunity effectiveness. This might reflect a need to manage *ACQOS*-mediated autoimmunity, which becomes significant under severe osmotic stress and dominates in stress acclimation conferred by pre-exposure to mild salinity. Our findings suggest that the genetic variability of certain *NLR* genes in *A. thaliana* populations is not only shaped by coevolution between plants and pathogens but also the need to balance responsiveness to biotic and abiotic stresses in the environment.

Figure legends

Figure 1

Identification of the *ACQOS* locus.

a, Acquired osmotolerance of *A. thaliana* accessions. Upper panel: A flow chart of the acquired osmotolerance assay. Middle panel: Salt tolerance when grown on soil. Three-week-old plants grown in pots were exposed to 500 mM NaCl in water for 49 d. Lower panel: Acquired osmotolerance. Salt-acclimated 2-week-old seedlings were mesh-transferred to MS agar plates containing 750 mM sorbitol for 21 d.

b, High-resolution mapping of the *ACQOS* locus using NILs. Upper panel: Acquired osmotolerance of Col-0, Bu-5, NIL-Col-0, and NIL-Bu-5. Lower panel: Graphical genotypes of NILs. Chromosomal segments of Col-0, off-white; Bu-5, green. Numbers above the genes are the last 3 digits of their Arabidopsis Genome Initiative (AGI) numbers (*At5g46XXX*).

c, Genome-wide association study for acquired osmotolerance. Upper panel: Manhattan plot of GWAS results for acquired osmotolerance. Middle panel: Close-up of the major GWAS peak in the vicinity of the *ACQOS* locus on chromosome 5. The position of the *ACQOS* gene is indicated by a red line. Lower panel: Linkage disequilibrium patterns within ± 500 kb upstream and downstream of the *ACQOS* locus.

d, Complementation test performed by transforming NIL-Bu-5 with *NLR4 (ACQOS)*. T_3 homozygous plants transformed with *native promoter: NLR4* (*ACQOS*) derived from Col-0 were used.

e, Acquired osmotolerance of *nlr2*, *nlr3-1*, and *nlr4-1* (*acqos-1*) mutants.

f, Expression of *ACQOS* in Col-0 plants under normal, salt acclimated, and subsequent osmotic stress conditions; gene expression was determined by qRT-PCR (mean ± se, *n* = 3).

g, Histochemical analysis of the expression pattern of *ACQOS* promoter: *GUS* in Col-0 seedlings grown under normal or osmotic stress conditions. GUS activities in two independent transgenic lines were measured using 4-MUG fluorometric assay. Differences between normal (white bars) and osmotic stress (black bars) conditions were analyzed by Student's t-test. (mean ± se, n = 7, ***P <0.001)

After salt acclimation, seedlings were grown in the presence of 750 mM sorbitol for 21 (**b**), 15 (**d**), or 20 (**e**) d. Similar results were obtained in three independent experiments; representative data are shown.

Figure 2

Haplotype diversity and functional evolution of the *ACQOS* locus.

a, Schematic representation of five haplogroups at the *ACQOS* locus, which differ by *NLR* tandem copy numbers and by nucleotide substitutions. Arrowheads below Group 2 *ACQOS* show nonsynonymous substitution compared to Group 1 *ACQOS*.

b, Relative frequencies of the five haplogroups among the 79 surveyed natural accessions.

c, Acquired osmotolerance of the five haplogroups. Salt-acclimated seedlings were grown in the presence of 750 mM sorbitol for 21 d.

d, Nucleotide diversity at all sites across the *ACQOS* locus (Groups 1 and 2). A dotted horizontal line indicates average genome-wide nucleotide diversity of *A. thaliana*[9].

e, Complementation test for acquired osmotolerance using Group 1 *ACQOS* (upper part) and Group 2 *ACQOS* (lower part). Salt-acclimated seedlings were grown in the presence of 750 mM sorbitol for 15 d. Arrowheads indicate T_2 seedlings with introduced Group 1 *ACQOS*.

f, Maximum-likelihood based phylogenetic tree of *NLR* genes in the *ACQOS* locus with three homologs from *Arabidopsis lyrata* as an outgroup. The values on the branches indicate the percentage of 1,000 bootstrap replicates.

Similar results of **Fig. 2c** and **2e** were obtained in at least three independent experiments; representative data are shown.

Figure 3

Contribution of *ACQOS* to immune responses and pathogen resistance after MAMP treatment.

a, Salicylic acid (SA) contents in Col-0 and NIL-Bu-5 plants under normal, salt stress, and subsequent osmotic stress conditions (mean ± se, $n = 3$).

b, Expression of *PR1*, *PR2*, and *EDS1* in Col-0 and NIL-Bu-5 plants under normal, salt stress, and subsequent osmotic stress conditions determined by qRT-PCR (mean ± se, $n = 3$). Differences between Col-0 and NIL-Bu-5 were analyzed by Student's t-test. *P <0.05; ***P <0.001.

c, Acquired osmotolerance of the immune signaling mutants *eds1-2*, *pad4-1*, and *npr1-1*[29], R protein accumulation and hence function mutants *rar1-21* and *sgt1b*[15], an SA-depleted *35S:nahG* transgenic plant[30], and the SA-deficient mutants *eds5-1*[31] (mutation in an SA transporter) and *sid2-2*[32] (mutation in isochorismate synthase). All the mutants were in the Col-0 background.

306 Similar results were obtained in three times independent experiments; representative
307 data are shown.
308 **d,** Chlorophyll content of immune deficient mutants as described in **c**.
309 Within each lines, bars with different letters are significantly different ($P < 0.01$,
310 one-way ANOVA with post-hoc Tukey HSD test, mean ± se, n=6).
311 **e**, Expression of *NHL10* and *PROPEP3* in Col-0, NIL-Bu-5 and *efr fls2* plants exposed
312 to 1 μM flg22 for 8h determined by qRT-PCR (mean ± se, $n = 3$).
313 **f,** Growth of syringe-infiltrated *Pst* DC3000 in rosette leaves of 4-week-old Col-0,
314 NIL-Bu-5 and *efr fls2* plants pretreated with water (Mock) or 1 μM flg22 for 24 h.
315 (mean ± se, $n = 5$). **e and f,** Differences between pretreatment with Mock and flg22
316 were analyzed by Student's t-test. *P <0.05; **P <0.01; ***P <0.001.
317
318
319

Supplementary Figure 1

Fine mapping of acquired osmotolerance.

Fine mapping was performed using 1993 osmo-sensitive F_2 (Col-0 × Bu-5) plants. The *ACQOS* locus exhibited strong linkage within approximately 100 kb between At5g_126 and At5g_136. The scores indicate recombination frequencies (%). The number under the markers shows the number of recombinants. *NLR* genes in the *ACQOS* locus are shown as colored arrows. Other genes are shown as black arrows.

Supplementary Figure 2

Chlorophyll contents for the acquired osmotolerant assays.

a. Chlorophyll contents of Col-0, NIL-Col-0, NIL-Bu-5 and Bu-5 as described in **Fig. 1b**.

b. Chlorophyll contents of accessions as described in **Fig. 2c**.

c. Chlorophyll contents of *acqos* complementation lines as described in **Fig. 2e**.

Within each lines, bars with different letters are significantly different ($P < 0.05$, one-way ANOVA with post-hoc Tukey HSD test, mean ± se, n=5-6).

Supplementary Figure 3

Graphical genotype of a BAC clone derived from the Bu-5 genome.

The BAC clone contained the entire 100-kb region (red line) narrowed down by fine mapping (see Supplementary Figure 1). *NLR* genes in the *ACQOS* locus are shown as colored arrows. Other genes are shown as gray arrows.

Supplementary Figure 4

Phenotypes of T_2 plants transformed with *native promoter : NLR^{Bu-5}* in Col-0 or *native promoter : $NLR3^{Col-0}$* in NIL-Bu-5.

a, Salt-acclimated 2-week-old seedlings were grown in the presence of 750 mM sorbitol for 12 days. None of the transgenic plants showed osmotolerance, indicating that *NLR^{Bu-5}* did not confer acquired osmotolerance. Experiments were repeated three times.

b, Chlorophyll contents of Col-0, NIL-Bu-5 and transgenic lines as described in **a** (mean ± se, n=6).

c. Expression levels of *NLR3* in NLR3_NIL-Bu-5 lines and *NIR^{Bu-5}* in NIR^{Bu-5}_Col-0 lines (mean ± se, n=3).

Supplementary Figure 5

Acquired osmotolerance of *NLR* T-DNA insertion mutants.

a, Schematic representation of the *ACQOS* locus and the sites of T-DNA insertions.

b, Salt-acclimated 2-week-old seedlings were grown in the presence of 750 mM sorbitol for 17 days. Only *acqos* knockout mutants showed the acquired osmotolerance. Experiments were repeated three times.

c, Chlorophyll content of each plants as described in **b**.

Within each lines, bars with different letters are significantly different ($P < 0.01$, one-way ANOVA with post-hoc Tukey HSD test, mean ± se, n=6).

d, Expression of the neighboring *NLRs* in the *acqos* mutatns. Expression levels were normalized to that of *β-actin* (mean ± se, $n = 3$).

Supplementary Figure 6

Phylogenetic tree of 104 Arabidopsis (Col-0) TIR-NLRs.

Phylogenetic tree was drawn using amino acid sequence of 104 TIR-NB-LRRs from Col-0. Red frame shows a magnified branch with tandem *NLR* genes (graphical genotypes) in the *ACQOS* locus.

Supplementary Figure 7

Acquired osmotolerance of plants overexpressing osmotic stress–inducible *ACQOS*$^{Col-0}$.

a and b, Relative *ACQOS* expression in T_3 plants under (**a**) normal growth conditions and (**b**) osmotic stress for 3 days. Expression levels were normalized to that of β*-actin* (mean ± se $n = 3$). Differences between Col-0 and the T_3 lines were analyzed by Student's *t*-test. ***P*<0.01, ****P* <0.001.

c, Phenotypes of T_3 homozygous plants with introduced *ACQOS*$^{Col-0}$. Salt-acclimated 2-week-old seedlings were grown in the presence of 750 mM sorbitol for 7 (upper panel) or 14 days (lower panel). Experiments were repeated three times.

d, Chlorophyll contents of *ACQOS*$^{Col-0}$ introduced lines as described in **c**. Within each lines, bars with different letters are significantly different ($P < 0.01$, one-way ANOVA with post-hoc Tukey HSD test, mean ± se, n=6).

Supplementary Figure 8

Phenotypes of F_1 progeny derived from a cross between Col-0 and NIL-Bu-5.

a, Osmotolerance of F_1 seedlings was intermediate between those of Col-0 and NIL-Bu-5, indicating that *ACQOS* reduces acquired osmotolerance. Experiments were repeated three times.

b, Chlorophyll contents of the F_1 plants after 14 days of osmotic stress (mean ± se, n = 4). Differences were analyzed by Student's t-test. $^{**}P < 0.01$, $^{***}P < 0.001$.

Supplementary Figure 9

Alignments of five *A. thaliana ACQOS* haplogroupes (Group 1-5) and *A. lyrata ACQOS* locus using Progressive MAUVE[33].

a. Alignments of five *A. thaliana ACQOS* haplogroupes (Group 1-5)

Regions of significant synteny between the species or groups are shown as colored blocks in the mauve alignment. Regions of sequence not shared between genotypes are seen as white gaps within the blocks or spaces between the blocks. Black bars and colored arrows show genes. Red bars show *TIR-NB-LRRs* used in **Fig. 2f**.

b. Alignments of the region around *ACQOS* locus between *A. thaliana* (Col-0) and *A. lyrata*.

Supplementary Figure 10

Polymorphism and divergence levels between Group 1 and 2 *ACQOS* genes.

Sliding window analysis of πa/πs in the coding region of Group 1 and 2 *ACQOS* genes. TIR, Toll/interleukin 1 receptor domain; NB, nucleotide-binding domain; Leucine-rich repeat domain.

Supplementary Figure 11

Phylogenetic trees of Group 1 *ACQOS*, Group 2 *ACQOS*, and Group 5 *NLR*.

To reveal phylogenetic relationships between the *ACQOS* genes of Groups 1 (blue) and 2 (orange) and the *NLR* genes of Group 5 (yellow), three maximum-likelihood

phylogenetic trees were drawn using different regions of the genes (shaded in gray in the upper panel). The graph showing nucleotide diversity of Group 1 and 2 *ACQOS* genes is identical to **Fig 2d**. The values on the branches indicate the percentage of 1,000 bootstrap replicates.

Supplementary Figure 12

Polymorphisms between the Group 5 *NLR* gene and Group 1 and 2 *ACQOS* genes.

The region of Group 5 *NLR* corresponding to the high-diversity region of *ACQOS* harbors two clearly distinct haplotypes, and Group 1 and 2 *ACQOS* are even closer to each haplotype of Group 5 *NLR*. See also **Supplementary Figure 11** Arrowheads indicate polymorphisms between the Group 5 *NLR* gene in some Group 5 accessions and Group 2 *ACQOS* gene.

Supplementary Figure 13

Group 3 *NLR3* is derived from Group 1 *NLR3* and *ACQOS* via gene deletion.

To reveal phylogenetic relationships between *NLR3* and *ACQOS* genes from Groups 1 (blue), 2 (orange), and 3 (green), maximum-likelihood phylogenetic trees were drawn using the indicated 5' and 3' regions of the genes. The values on the branches indicate the percentage of 1,000 bootstrap replicates.

Supplementary Figure 14

Effect of temperature on acquired osmotolerance in Col-0 and NIL-Bu-5.

Salt-acclimated seedlings grown under normal conditions (22 ºC) were transferred to plates containing 750 mM sorbitol and grown at 22 ºC (control) or 28 ºC for 8 days.

Experiments were repeated three times.

Supplementary Figure 15

ABA is dispensable for acquired osmotolerance in absence of ACQOS.

a, ABA contents in Col-0 and NIL-Bu-5 (mean ± se, $n = 3$).

b, Expression profiles of the ABA responsible genes *RAB18* and *Raffinose synthase 6* (*RS6*), and the ABA synthesis gene *NCED3* in Col-0 and NIL-Bu-5 (mean ± se, $n = 3$).

c, Acquired osmotolerance of Col-0 and NIL-Bu-5 carrying mutations in the ABA signaling component gene *ABI1* (*abi1-1*_Col-0 and *abi1-1*_NIL-Bu-5) or the ABA biosynthesis genes *ABA2* (*aba2-1*_Col-0 and *aba2-1*_NIL-Bu-5), and *NCED3* (*ncde3-2*_Col-0 and *ncde3-2*_NIL-Bu-5). After salt acclimation, seedlings were grown in the presence of 750 mM sorbitol for 21 days. Experiments were repeated three times.

Supplementary Figure 16

Immunoblot analysis for FLS2 and BAK1.

Ten-day-old seedlings of Col-0, NIL-Bu-5, *acqos-1*, *acqos-2*, *bak1-4* and *efr fls2* under normal growth conditions were subjected to immunoblot analysis with the indicated antibodies. Equal loading of protein lysates was verified by Ponceau S staining of the protein blots. There were no significant alterations in FLS2 and BAK1 accumulation among Col-0, NIL-Bu-5 and *acqos* mutants.

Supplementary Figure 17

Osmotolerance after acclimation with mild osmotic stress.

a. Plants acclimated with 150 mM sorbitol were grown in the presence of 750 mM sorbitol for 14 days. As well as salt-acclimation, Bu-5, NIL-Bu-5 and *acqos-1* showed osmotolerance, whereas Col-0 plants did not. Experiments were repeated three times. **b.** Chlorophyll content of each plants as described in **a**. Within each line, bars with different letters are significantly different ($P < 0.05$, one-way ANOVA with post-hoc Tukey HSD test, mean ± se, n=6).

Methods

Plant material and growth conditions

Arabidopsis seeds were sown on agar (0.8%, w/v) plates containing full-strength Murashige and Skoog (MS) salts with a vitamin mixture (10 mg l^{-1} myoinositol, 200 μg l^{-1} glycine, 50 μg l^{-1} nicotinic acid, 50 μg l^{-1} pyridoxine hydrochloride, 10 μg l^{-1} thiamine hydrochloride, pH 5.7) and 1% sucrose. Plates were sealed with surgical tape; the seeds were stratified at 4 ºC for 4–7 days and then transferred to a growth chamber (80 μmol photons m^2 s^{-1}; 16 h/8 h light/dark cycle; 22 ºC) for germination and growth. Seeds of the following Arabidopsis mutants were obtained from the Arabidopsis Biological Resource Center (Ohio State University): *acqos* (SALK_122941, SALK_072727), *nlr2* (SALK_147652C), *nlr3* (SALK_145278, SALK_097845), *aba2-1* (CS156), *abi1-1* (CS22), *pad4-1* (CS3806), *sid2-2* (CS16438), *eds5-1* (CS3735), and *npr1-1* (CS3726). The *eds1-2* mutant[34] and *35S:NahG* transgenic line[30] were described previously. The *nced3-2* mutant[19] was kindly provided by Dr. Kaoru Urano. To generate *aba2-1*_NIL-Bu-5 and *nced3-2*_NIL-Bu-5, *aba2-1* and *nced3-2* mutants were crossed with NIL-Bu-5 (see below), respectively. To identify the homozygous of each mutations and *ACQOS* locus, the F_2 seedlings were genotyped by sequencing or SSLP markers (**Supplementary Table 2**). The F3 progeny was used in this study. To generate *abi1-1*_Col-0 and *abi1-1*_NIL-Bu-5, *abi1-1* (Ler background) was backcrossed three times to Col-0 or NIL-Bu-5.

Stress treatment for acquired osmotolerance assay

7-day-old seedlings grown on nylon mesh on an MS agar plate were mesh-transferred to a plate supplemented with 100 mM NaCl for 7 d. The 14-day-old seedlings were then

mesh transferred to a plate supplemented with 750mM sorbitol for 14 d. Mild osmotic stress (e.g. 150 mM sorbitol) is able to induce the acquired osmotolerance as well as the mild NaCl stress does (**Supplementary Fig. 17**).

High-resolution mapping of *ACQOS*

BC_5F_2 plants were generated by backcrossing F_2 plants (derived from a cross between Bu-5 and Col-0 and showing acquired salt tolerance) to Col-0 plants five times. We screened the BC_5F_2 plants for recombination events within the mapped 100-kb region containing *ACQOS*. We also developed two near-isogenic lines, named NIL-Col-0 and NIL-Bu-5, which carried a small chromosomal segment from Bu-5 containing the *ACQOS* region in the genetic background of Col-0. Genotyping was performed with SSLP markers and using SNP detection by sequencing (**Supplementary Table 1**).

Genome-wide association study

A GWAS was performed to find loci associated with the absence or presence of acquired osmotolerance in 179 worldwide natural accessions (**Supplementary Table 1**). Of 350 accessions analyzed in this study, 250k SNP dataset is available only for 173 accessions. We excluded some accessions whose phenotype is not penetrated (e.g., a within line variation), and added some accessions obtained from ABRC. As for the GWAS, the osmotolerance phenotype was scored in a binary (absent or present) way because this "all or nothing" difference of the phenotype was so clear. We used the 250k SNP data as a genotype set[35]. To deal with the confounding effect of population structure, we employed a mixed model incorporating a genome-wide kinship matrix as a

519 random effect[36]. We used the GWAPP platform[37] to perform GWAS and to generate the
520 Manhattan and linkage disequilibrium plots.
521
522 **Generation of a BAC library from the Bu-5 genome and sequencing of the *ACQOS***
523 **locus**
524 A BAC library derived from the Bu-5 genome was generated by Amplicon Express
525 (USA). BAC clones were extracted with a NucleoBond BAC 100 kit (Macherey-Nagel)
526 and sequenced. The *ACQOS* loci of 79 accessions (**Supplementary Table 3**) were
527 amplified using a haplogroup-specific primer set (**Supplementary Table 4**), the PCR
528 fragments were cloned into pCR-TOPO (Invitrogen) and sequenced.
529
530 **Plasmid construction and transformation**
531 For complementation analysis, the genomic region of each *NLR* (2.0 kb upstream of the
532 ATG initiation codon and 1.0 kb downstream region as a terminator in the *ACQOS*
533 locus of Col-0) were amplified by PCR with AscI linker primers and cloned into the
534 AscI sites introduced into the binary vectors pGreen0029 and pGreen0129. The *ACQOS*
535 *promoter: GUS* plasmid was constructed by amplifying a 2.0-kb DNA fragment
536 upstream of the *ACQOS* initiation codon by PCR and cloning it into the BamHI site of
537 pBI101.
538 All constructs were introduced into *Agrobacterium tumefaciens* strain GV3101 carrying
539 pSoup, a helper plasmid necessary for pGreen replication[38]. Agrobacteria were then
540 used for plant transformation by the floral dip method. Primers for cloning are listed in
541 **Supplementary Table 5**. Transgenic plants were selected on MS agar plates containing

200 μg ml^{-1} claforan and 25 μg ml^{-1} kanamycin or 20 μg ml^{-1} hygromycin. Ten-day-old seedlings (T_1 plants) were transferred to the soil pots.

Quantitative RT-PCR

Total RNA (2 μg) was isolated with an RNeasy Plant Mini Kit (QIAGEN), treated with DNase I (Invitrogen) and used as a template to synthesize first-strand cDNA using SuperScript II Reverse Transcriptase (Invitrogen) and an oligo dT primer. qRT-PCR was performed using a LightCycler 96 (Roche Diagnostics) with FastStart Essential DNA Green Master (Roche Diagnostics) in a total volume of 12 μL under the following conditions: 95 ºC for 10 min followed by 45–50 cycles of 95 ºC for 20 s, 54 ºC for 20 s, and 72 ºC for 20 s. *β-Actin* was used as an internal standard. Primers and their efficiencies are listed in **Supplementary Table 6**.

GUS staining and quantification

ACQOS promoter: GUS transgenic seedlings were salt-acclimated under 100 mM NaCl for 7 days and subsequently subjected to 750 mM sorbitol for 7 days. Seedlings were then washed twice with phosphate buffer and incubated in GUS buffer (10 mM phosphate buffer [pH 7], 0.5% Triton X-100, 1 mg ml-1 X-Gluc, 2 mM potassium ferricyanide) for 3–5 h at 37 ºC. Chlorophyll was subsequently removed by incubation in 100% ethanol. Quantification of GUS activity was performed according to 4-MUG fluorometric assay[39]. Transgenic seedlings with or without osmotic stress were homogenized with GUS extraction buffer (100 mM Sodium phosphate, 10 mM EDTA, 10 mM DTT, 0.1% Triton X-100, 20 % Methanol and 1 mM 4-MUG) and incubated at 37 ºC for 60 min. After incubation, 100 μL of each samples were mixed with 4 mL 200

mM Na_2CO_3 and 4-MU fluorescence was measured with excitation at 365 nm, emission at 455 nm on a spectrofluorimeter. Fluorescence intensity was calculated using 4-MU standards (0.001~1 mM). Then GUS activity was normalized with protein concentration quantified with Bradford (Bio-Rad).

Population genetic analysis

DnaSP v.5 was used to calculate nucleotide diversity and $\pi a/\pi s$[40]. In the sliding window analysis, window length was 100 bp and step size was 25 bp. We generated phylogenetic trees using the maximum-likelihood method implemented in the MEGA5 software[41].

Analysis of plant hormone contents

About 100 mg (fresh weight) of tissues were subjected to hormone quantification. The hormone extraction and fractionation were performed using the method described previously[42]. Hormones were measured with an UPLC-ESI-qMS/MS (AQUITY UPLC™ System/Xevo-TQS; Waters) with an ODS column (AQUITY UPLC BEH C_{18} , 1.7 μm, 2.1 × 100 mm, Waters)[42].

Bacterial inoculation assays

Bacterial inoculation assays were performed as described previously[43] with the following modifications. Following 1 μM flg22 or water (mock) pretreatment for 24 h, *Pst* DC3000 suspension at 1 x 10^5 cfu/mL was syringe-infiltrated into 3 leaves of 5 plants per genotype per treatment. Three days after inoculation, these leaves were collected and then their fresh weight was determined before the quantification of leaf

bacteria using leaf fresh weight (g) for normalization. These experiments (5 replicates each) have been repeated three times with the same conclusions.

Immunoblot analysis

Ten-day-old seedlings were subjected to immunoblot analysis with the indicated antibodies, essentially as described previously[44]. Equal loading of protein lysates was verified by Ponceau S staining of the protein blots.

Data availability

DNA sequences that support the findings of this work have been deposited to DNA Data Bank of Japan (DDBJ) with the following accession numbers: ACQOS_Col-0 (LC214887), ACQOS_Rou-0 (LC214888), ACQOS_ Zu-0 (LC214889), ACQOS_ Kl-1 (LC214890), ACQOS_ Van-0 (LC214891), ACQOS_ Bu-5 (LC214892), ACQOS_ C24 (LC214893), and ACQOS_ Bs-1 (LC214894). The data are available from the National Center for Biotechnology Information (NCBI).

606 **References**

607 1. Sung, D.Y., Kaplan, F., Lee, K.J. & Guy, C.L. Acquired tolerance to
608 temperature extremes. *Trends Plant Sci* **8**, 179-87 (2003).
609 2. Katori, T. *et al.* Dissecting the genetic control of natural variation in
610 salt tolerance of *Arabidopsis thaliana* accessions. *J Exp Bot* **61**,
611 1125-38 (2010).
612 3. Kim, T.H. *et al.* Natural variation in small molecule-induced
613 TIR-NB-LRR signaling induces root growth arrest via EDS1- and
614 PAD4-complexed R protein VICTR in Arabidopsis. *Plant Cell* **24**,
615 5177-92 (2012).
616 4. Weigel, D. Natural variation in Arabidopsis: from molecular genetics
617 to ecological genomics. *Plant Physiol* **158**, 2-22 (2012).
618 5. Mitchell-Olds, T. & Schmitt, J. Genetic mechanisms and evolutionary
619 significance of natural variation in Arabidopsis. *Nature* **441**, 947-52
620 (2006).
621 6. Kim, T.H. *et al.* Chemical genetics reveals negative regulation of
622 abscisic acid signaling by a plant immune response pathway. *Curr*
623 *Biol* **21**, 990-7 (2011).
624 7. Maekawa, T., Kufer, T.A. & Schulze-Lefert, P. NLR functions in plant
625 and animal immune systems: so far and yet so close. *Nat Immunol* **12**,
626 817-26 (2011).
627 8. Shao, Z.Q. *et al.* Large-Scale Analyses of Angiosperm
628 Nucleotide-Binding Site-Leucine-Rich Repeat Genes Reveal Three
629 Anciently Diverged Classes with Distinct Evolutionary Patterns.
630 *Plant Physiol* **170**, 2095-109 (2016).
631 9. Nordborg, M. *et al.* The pattern of polymorphism in *Arabidopsis*
632 *thaliana*. *PLoS Biology* **3**, e196 (2005).
633 10. Shirano, Y., Kachroo, P., Shah, J. & Klessig, D.F. A gain-of-function
634 mutation in an Arabidopsis Toll Interleukin1 receptor-nucleotide
635 binding site-leucine-rich repeat type R gene triggers defense
636 responses and results in enhanced disease resistance. *Plant Cell* **14**,
637 3149-3162 (2002).
638 11. Cui, H. *et al.* A core function of EDS1 with PAD4 is to protect the
639 salicylic acid defense sector in Arabidopsis immunity. *New Phytol* **213**,
640 1802-1817 (2017).
641 12. Zhang, Y., Goritschnig, S., Dong, X. & Li, X. A gain-of-function
642 mutation in a plant disease resistance gene leads to constitutive
643 activation of downstream signal transduction pathways in *suppressor*
644 *of npr1-1, constitutive 1*. *Plant Cell* **15**, 2636-46 (2003).
645 13. Yasuda, M. *et al.* Antagonistic interaction between systemic acquired
646 resistance and the abscisic acid-mediated abiotic stress response in
647 Arabidopsis. *Plant Cell* **20**, 1678-92 (2008).

14. Alcázar, R. & Parker, J.E. The impact of temperature on balancing immune responsiveness and growth in Arabidopsis. *Trends Plant Sci* **16**, 666-75 (2011).
15. Shirasu, K. The HSP90-SGT1 chaperone complex for NLR immune sensors. *Annu Rev Plant Biol* **60**, 139-64 (2009).
16. Huang, X., Li, J., Bao, F., Zhang, X. & Yang, S. A gain-of-function mutation in the Arabidopsis disease resistance gene *RPP4* confers sensitivity to low temperature. *Plant Physiol* **154**, 796-809 (2010).
17. Yang, H. *et al.* A mutant CHS3 protein with TIR-NB-LRR-LIM domains modulates growth, cell death and freezing tolerance in a temperature-dependent manner in Arabidopsis. *Plant J* **63**, 283-96 (2010).
18. Léon-Kloosterziel, K.M. *et al.* Isolation and characterization of abscisic acid-deficient Arabidopsis mutants at two new loci. *Plant Journal* **10**, 655-661 (1996).
19. Urano, K. *et al.* Characterization of the ABA-regulated global responses to dehydration in Arabidopsis by metabolomics. *Plant J* **57**, 1065-78 (2009).
20. Leung, J. *et al.* Arabidopsis ABA response gene ABI1: features of a calcium-modulated protein phosphatase. *Science* **264**, 1448-52 (1994).
21. Meyer, K., Leube, M.P. & Grill, E. A protein phosphatase 2C involved in ABA signal transduction in Arabidopsis thaliana. *Science* **264**, 1452-5 (1994).
22. Bostock, R.M., Pye, M.F. & Roubtsova, T.V. Predisposition in plant disease: exploiting the nexus in abiotic and biotic stress perception and response. *Annu Rev Phytopathol* **52**, 517-49 (2014).
23. Ahmad, S. *et al.* Genetic dissection of basal defence responsiveness in accessions of Arabidopsis thaliana. *Plant Cell Environ* **34**, 1191-206 (2011).
24. Boller, T. & Felix, G. A renaissance of elicitors: perception of microbe-associated molecular patterns and danger signals by pattern-recognition receptors. *Annu Rev Plant Biol* **60**, 379-406 (2009).
25. Vetter, M.M. *et al.* Flagellin perception varies quantitatively in *Arabidopsis thaliana* and its relatives. *Mol Biol Evol* **29**, 1655-67 (2012).
26. Jeworutzki, E. *et al.* Early signaling through the Arabidopsis pattern recognition receptors FLS2 and EFR involves Ca-associated opening of plasma membrane anion channels. *Plant J* **62**, 367-78 (2010).
27. Sun, Y. *et al.* Structural basis for flg22-induced activation of the Arabidopsis FLS2-BAK1 immune complex. *Science* **342**, 624-8 (2013).
28. Zipfel, C. *et al.* Bacterial disease resistance in Arabidopsis through flagellin perception. *Nature* **428**, 764-767 (2004).

29. Cao, H., Bowling, S.A., Gordon, A.S. & Dong, X. Characterization of an Arabidopsis Mutant That Is Nonresponsive to Inducers of Systemic Acquired Resistance. *Plant Cell* **6**, 1583-1592 (1994).
30. Reuber, T.L. *et al.* Correlation of defense gene induction defects with powdery mildew susceptibility in Arabidopsis enhanced disease susceptibility mutants. *Plant Journal* **16**, 473-485 (1988).
31. M C Wildermuth, J.D., G Wu, and F M Ausubel. Isochorismate synthase is required to synthesize salicylic acid for plant defence. *Nature* **414**, 562-565 (2001).
32. Rogers, E.E. & Ausubel, F.M. Arabidopsis enhanced disease susceptibility mutants exhibit enhanced susceptibility to several bacterial pathogens and alterations in PR-1 gene expression. *Plant Cell* **9**, 305-316 (1997).
33. Darling, A.E., Mau, B. & Perna, N.T. progressiveMauve: Multiple Genome Alignment with Gene Gain, Loss and Rearrangement. *PLoS One* **5**, e11147 (2010).
34. Bartsch, M. *et al.* Salicylic acid-independent *ENHANCED DISEASE SUSCEPTIBILITY1* signaling in Arabidopsis immunity and cell death is regulated by the monooxygenase *FMO1* and the Nudix hydrolase *NUDT7*. *Plant Cell* **18**, 1038-51 (2006).
35. Horton, M.W. *et al.* Genome-wide patterns of genetic variation in worldwide Arabidopsis thaliana accessions from the RegMap panel. *Nat Genet* **44**, 212-6 (2012).
36. Atwell, S. *et al.* Genome-wide association study of 107 phenotypes in *Arabidopsis thaliana* inbred lines. *Nature* **465**, 627-31 (2010).
37. Seren, U. *et al.* GWAPP: A Web Application for Genome-Wide Association Mapping in Arabidopsis. *Plant Cell* **24**, 4793-805 (2012).
38. Hellens, R.P., Edwards, E.A., Leyland, N.R., Bean, S. & Mullineaux, P.M. pGreen: a versatile and flexible binary Ti vector for *Agrobacterium*-mediated plant transformation. *Plant Molecular Biology* **42**, 819-832 (2000).
39. Jefferson, R.A., Kavanagh, T.A. & Bevan, M.W. GUS fusions: ß-glucuronidase as a sensitive and versatile gene fusion marker in higher plants. *EMBO Journal* **6**, 3901-3907 (1987).
40. Librado, P. & Rozas, J. DnaSP v5: a software for comprehensive analysis of DNA polymorphism data. *Bioinformatics* **25**, 1451-2 (2009).
41. Tamura, K. *et al.* MEGA5: molecular evolutionary genetics analysis using maximum likelihood, evolutionary distance, and maximum parsimony methods. *Mol Biol Evol* **28**, 2731-9 (2011).
42. Kojima, M. & Sakakibara, H. Highly sensitive high-throughput profiling of six phytohormones using MS-probe modification and liquid chromatography-tandem mass spectrometry. *Methods Mol Biol* **918**, 151-64 (2012).

43. Lu, X. *et al.* Uncoupling of sustained MAMP receptor signaling from early outputs in an Arabidopsis endoplasmic reticulum glucosidase II allele. *Proc Natl Acad Sci U S A* **106**, 22522-7 (2009).
44. Yamada, K., Saijo, Y., Nakagami, H. & Takano, Y. Regulation of sugar transporter activity for antibacterial defense in *Arabidopsis*. *Science* **354**, 1427-1430 (2016).

Supplementary information is available in the online version of the paper.

Acknowledgements

We thank Marcel von Reth of the Department of Plant-Microbe Interactions, Max Planck Institute for Plant Breeding Research, for technical assistance. We gratefully acknowledge Kaoru Urano of RIKEN CSRS for providing seed. The Arabidopsis accessions used in this study are maintained and provided by the RIKEN BRC through the National Bio-Resource Project of the MEXT, Japan. This work was supported by JSPS KAKENHI Grant Numbers JP25119722 (to T.Taji), JP15K07845 (to T.Taji), JP14J07115 (to H.A.), JP26291062 and 16H01469 (to Y.Saijo), Strategic Young Researcher Overseas Visits Program for Accelerating Brain Circulation of JSPS (No. S2306 to T. Taji), JST PRESTO (JPMJPR13B6 to Y.Saijo) and a Deutsche Forschungsgemeinschaft CRC 680 grant (to J.E.P and R.A.).

Author contributions

H.A. and T. Taji initiated, conceived and coordinated the project; H.A., identified *ACQOS* locus and characterized plants altered with the *ACQOS* locus; T.K., generated NIL plants; T. Tsuchimatsu performed population genetic analyses; T. Tsuchimatsu, O.H., A.E.L., Y. Kobayashi and M.A.G. performed GWAS; T. Hirase, Y.T. and Y.

Saijo designed and performed defence-related assays; H.S. and M.K. determined SA and ABA contents; S.I. and M.K. provided *A. thaliana* accession seeds and their markers; J.E.P., R.A., M.K., K.S., T.Hayashi, Y. Sakata and Y. Saijo supervised the project; T. Taji and Y. Saijo wrote the manuscript with assistance from T. Tsuchimatsu, J.E.P., R.A., M.K., K.S., and Y. Sakata.

Author information

The authors declare no competing financial interests. Readers are welcome to comment on the online version of the paper. Correspondence and requests for materials should be addressed to T.Taji (t3teruak@nodai.ac.jp).

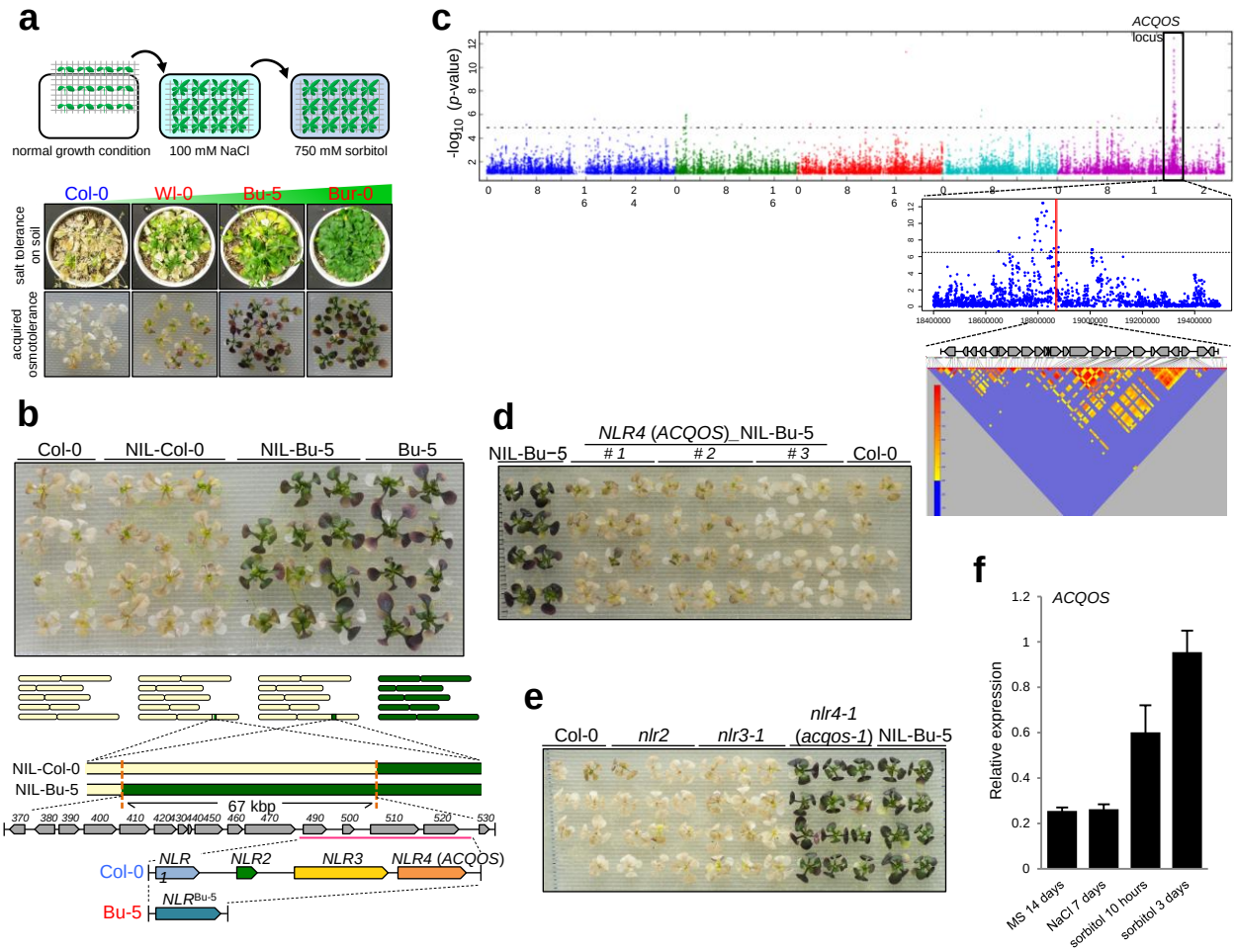

Figure 1
Identification of the *ACQOS* locus.

a, Acquired osmotolerance of *A. thaliana* accessions. Upper panel: A flow chart of the acquired osmotolerance assay. Middle panel: Salt tolerance when grown on soil. Three-week-old plants grown in pots were exposed to 500 mM NaCl in water for 49 d. Lower panel: Acquired osmotolerance. Salt-acclimated 2-week-old seedlings were mesh-transferred to MS agar plates containing 750 mM sorbitol for 21 d.
b, High-resolution mapping of the *ACQOS* locus using NILs . Upper panel: Acquired osmotolerance of Col-0, Bu-5, NIL-Col-0, and NIL- Bu-5. Lower panel: Graphical genotypes of NILs. Chromosomal segments of Col-0, off-white; Bu-5, green. Numbers above the genes are the last 3 digits of their Arabidopsis Genome Initiative (AGI) numbers (*At5g46XXX*).
c, Genome-wide association study for acquired osmotolerance. Upper panel: Manhattan plot of GWAS results for acquired osmotolerance. Middle panel: Close-up of the major GWAS peak in the vicinity of the *ACQOS* locus on chromosome 5. The position of the *ACQOS* gene is indicated by a red line. Lower panel: Linkage disequilibrium patterns within ± 500 kb upstream and downstream of the *ACQOS* locus.
d, Complementation test performed by transforming NIL-Bu-5 with *NLR4 (ACQOS)*. T_3 homozygous plants transformed with *native promoter: NLR4* (*ACQOS*) derived from Col-0 were used.
e, Acquired osmotolerance of *nlr2*, *nlr3-1*, and *nlr4-1* (*acqos-1*) mutants.
f, Expression of *ACQOS* in Col-0 plants under normal, salt acclimated, and subsequent osmotic stress conditions; gene expression was determined by qRT-PCR (mean ± se, *n* = 3).
g, Histochemical analysis of the expression pattern of *ACQOS* promoter: *GUS* in Col-0 seedlings grown under normal or osmotic stress conditions. GUS activities in two independent transgenic lines were measured using 4-MUG fluorometric assay. Differences between normal (white bars) and osmotic stress (black bars) conditions were analyzed by Student's t-test. (mean ± se, n = 7, ***P <0.001)
After salt acclimation, seedlings were grown in the presence of 750 mM sorbitol for 21 (**b**), 15 (**d**), or 20 (**e**) d. Similar results were obtained in three independent experiments; representative data are shown.

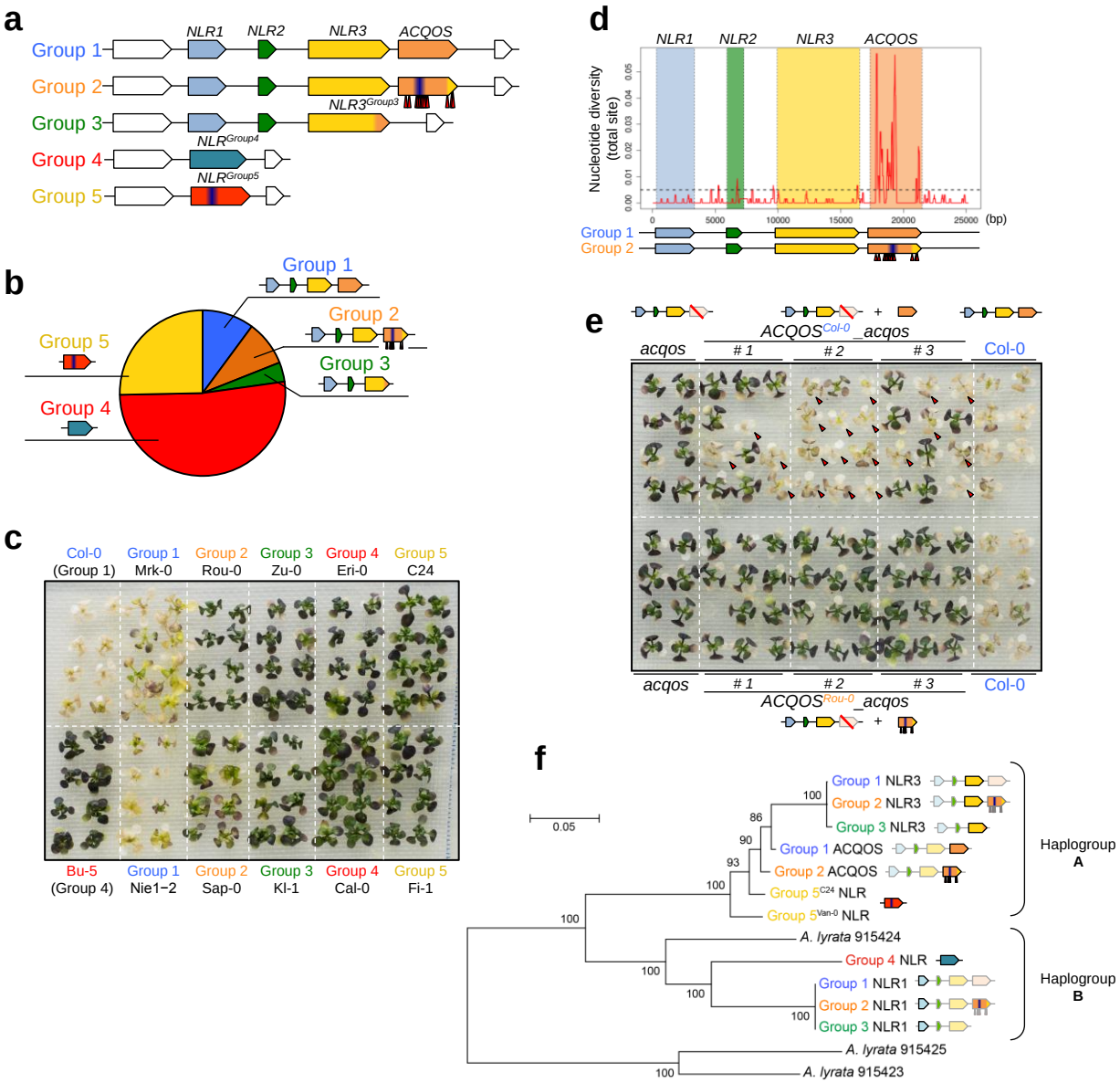

Figure 2
Haplotype diversity and functional evolution of the *ACQOS* locus.

a, Schematic representation of five haplogroups at the *ACQOS* locus, which differ by *NLR* tandem copy numbers and by nucleotide substitutions. Arrowheads below Group 2 *ACQOS* show nonsynonymous substitution compared to Group 1 *ACQOS*.
b, Relative frequencies of the five haplogroups among the 79 surveyed natural accessions.
c, Acquired osmotolerance of the five haplogroups . Salt-acclimated seedlings were grown in the presence of 750 mM sorbitol for 21 d.
d, Nucleotide diversity at all sites across the *ACQOS* locus (Groups 1 and 2). A dotted horizontal line indicates average genome-wide nucleotide diversity of *A. thaliana* (Nordborg et al. 2005).
e, Complementation test for acquired osmotolerance using Group 1 *ACQOS* (upper part) and Group 2 *ACQOS* (lower part) . Salt-acclimated seedlings were grown in the presence of 750 mM sorbitol for 15 d. Arrowheads indicate T_2 seedlings with introduced Group 1 *ACQOS*.
f, Maximum-likelihood based phylogenetic tree of *NLR* genes in the *ACQOS* locus with three homologs from *Arabidopsis lyrata* as an outgroup. The values on the branches indicate the percentage of 1,000 bootstrap replicates.
Similar results of **Fig. 2c** and **2e** were obtained in at least three times independent experiments; representative data are shown.

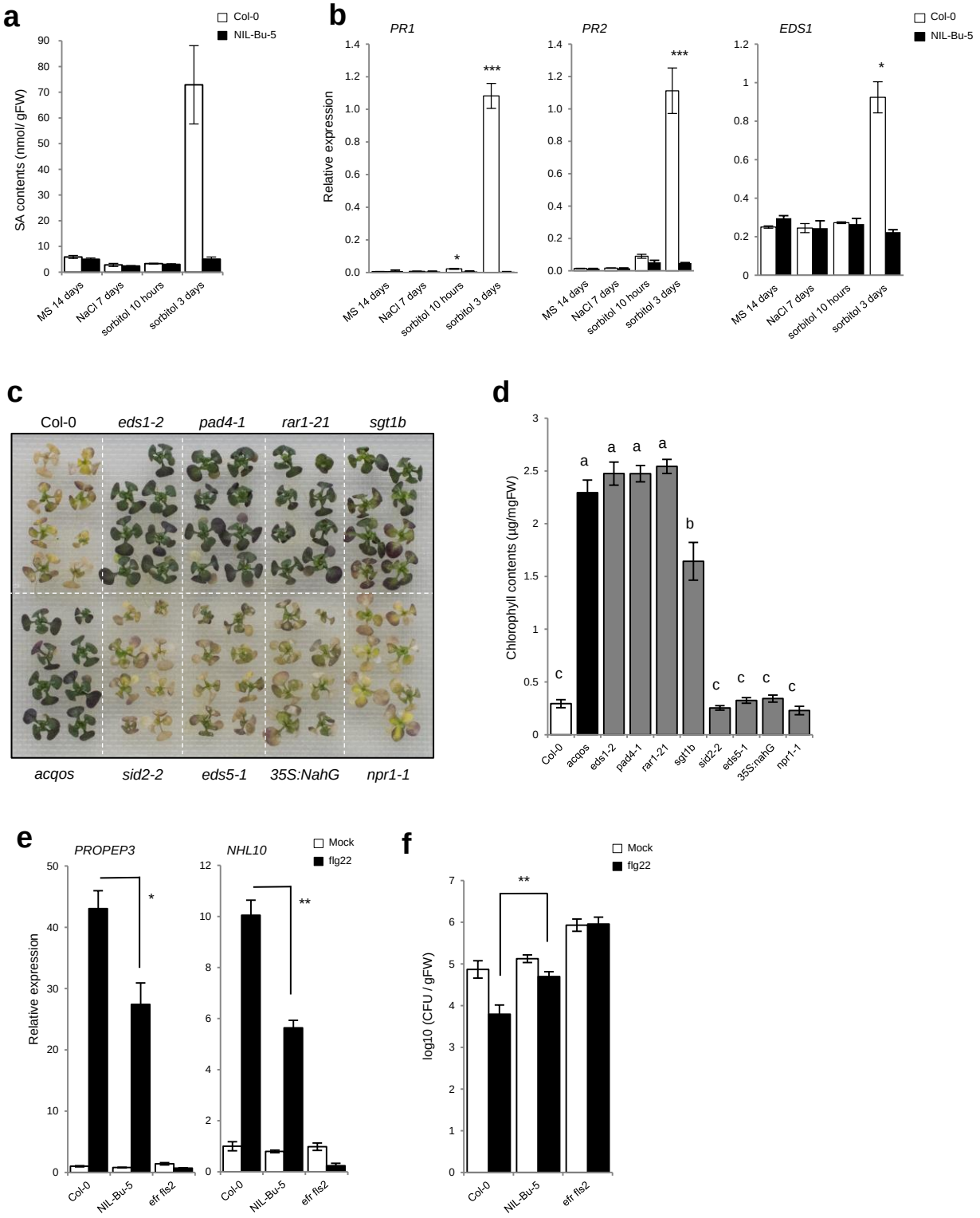

Figure 3
Contribution of *ACQOS* to immune responses and pathogen-resistance after MAMP treatment.

a, Salicylic acid (SA) contents in Col-0 and NIL-Bu-5 plants under normal, salt stress, and subsequent osmotic stress conditions.
b, Expression of *PR1*, *PR2*, and *EDS1* in Col-0 and NIL-Bu-5 plants under normal, salt stress, and subsequent osmotic stress conditions determined by qRT-PCR (mean ± se , $n = 3$). Differences between Col-0 and NIL-Bu-5 were analyzed by Student's t-test. *P <0.05; ***P <0.001.
c, Acquired osmotolerance of the immune signaling mutants *eds1-2*, *pad4-1*, and *npr1-1*[28], R protein accumulation and hence function mutants *rar1-21* and *sgt1b*14, an SA-depleted *35S:nahG* transgenic plant29, and the SA-deficient mutants *eds5-1*[30] (mutation in an SA transporter) and *sid2-2*[31] (mutation in isochorismate synthase). All the mutants were in the Col-0 background.
Similar results were obtained in three times independent experiments; representative data are shown.
d, Chlorophyll content of immune deficient mutants as described in **c**.
Within each lines, bars with different letters are significantly different (P < 0.01, one-way ANOVA with post-hoc Tukey HSD test, mean ± se, n=6).
e, Expression of *NHL10* and *PROPEP3* in Col-0, NIL-Bu-5 and *efr fls2* plants exposed to water (Mock) or 1 mM flg22 for 8h determined by qRT-PCR (mean ± se, $n = 3$).
f, Growth of syringe-infiltrated *Pst* DC3000 in rosette leaves of 4-week-old Col-0, NIL-Bu-5 and *efr fls2* plants pretreated with water (Mock) or 1 mM flg22 for 24 h. (mean ± se, $n = 5$). **e and f,** Differences between samples were analyzed by Student's t-test. *P <0.05; **P <0.01.